sustainability

MDPI

Article

Study on the Dust Content in Dead-End Drifts in the Potash Mines for Various Ventilation Modes

Aleksey Isaevich [1], Mikhail Semin [1,*], Lev Levin [1], Andrey Ivantsov [2] and Tatyana Lyubimova [2]

[1] Mining Institute of the Ural Branch of the Russian Academy of Sciences, 614007 Perm, Russia; aero_alex@mail.ru (A.I.); aerolog_lev@mail.ru (L.L.)
[2] Institute of Continuous Media Mechanics of the Ural Branch of the Russian Academy of Sciences Perm, 614013 Perm, Russia; aivantsov@gmail.com (A.I.); lyubimovat@mail.ru (T.L.)
* Correspondence: seminma@inbox.ru

Abstract: This article deals with the reduction of dust content in the working areas of potash mines in the conditions of operating combines. This problem is topical, since the high dust concentrations in the atmosphere of dead-end drifts lead to the development of occupational diseases among miners, and traditional methods of dust control are often unsuitable for potash salts conditions. We describe the results of experimental studies carried out for the potash mine of the Verkhnekamskoye potassium-magnesium salt deposit. Next, a mathematical model of the dust–air mixture dynamics is formulated and parametrized. The Euler–Euler approach and the model of a homogeneous multicomponent medium are used. The results of a simulation for two ventilation systems (forced and exhaust) are presented. Several options for air flow rates are considered. A conclusion is reached about the most effective parameters of ventilation systems, which allows for minimizing the concentration of dust in the zone of the combine driver.

Keywords: mine ventilation; industrial safety; dust; salt aerosol; mathematical modeling; multiphase flows

check for updates

Citation: Isaevich, A.; Semin, M.; Levin, L.; Ivantsov, A.; Lyubimova, T. Study on the Dust Content in Dead-End Drifts in the Potash Mines for Various Ventilation Modes. *Sustainability* **2022**, *14*, 3030. https://doi.org/10.3390/su14053030

Academic Editor: Chongchong Qi

Received: 9 February 2022
Accepted: 1 March 2022
Published: 4 March 2022

Publisher's Note: MDPI stays neutral with regard to jurisdictional claims in published maps and institutional affiliations.

Copyright: © 2022 by the authors. Licensee MDPI, Basel, Switzerland. This article is an open access article distributed under the terms and conditions of the Creative Commons Attribution (CC BY) license (https://creativecommons.org/licenses/by/4.0/).

1. Introduction

The major operations performed in the process of underground mining are the destruction of the rock mass, its loading, and transportation through the system of mine workings to the surface. These operations lead to the formation of both rather large fragments of rocks (including oversized fragments) and a large amount of dusty fraction. The latter is easily transported by air flow through the mine workings and can lead to unacceptably high dust content in the atmosphere of these workings during mining operations.

In sufficient concentrations, dust in the atmosphere of mine workings is an unfavorable factor in mining operations and can represent a serious hazard. For example, coal dust is explosive [1,2]. Over time, the daily prolonged stays of miners in the working areas of coal mines with a high dust content leads to the development of such occupational diseases as chronic bronchitis, pneumoconiosis, and silicosis [3,4]. Similar problems related to the impact of dust on the health of miners exist in potash mines [5]. Miners who regularly spend time in the dusty working areas of potash mines eventually develop such specific diseases as subatrophic rhinitis, pharyngitis, ulceration of the nasal mucosa, phlegmon, chronic bronchitis, et cetera.

In this article, we will focus on the dustiness of potash mines. It is known from experimental studies that the concentration of dust in dead-end drifts in potash mines can exceed 2000 mg/m^3 [6,7]. At the same time, according to safety rules in Russia and the CIS countries, the maximum permissible concentration of salt dust is only 5 mg/m^3. As such, it is important to control the dust content of the atmosphere of potash mines, along with other properties of the air in mine workings (gas concentrations, temperature, and relative humidity) [8,9].

There are many studies in the existing literature related to dust control; however, most focus on coal mines. Regarding coal mines, there have been purely experimental studies [10,11] and theoretical calculations [2,12,13], as well as complex experimental and theoretical studies, including the calibration of CFD models for the transfer of harmful impurities according to experimental data [9,14]. In [15], new methods and approaches were developed for experimental monitoring of coal dust concentrations. In [9], the optimal air velocity for ventilation of a dead-end face was investigated in terms of minimizing the concentration of coal dust. In [14,16] the authors considered the use of irrigation to minimize the concentration of coal dust.

At the same time, studies of the dust content of the atmosphere of potash mines are nearly absent from the literature. This is logical given that potash dust is generally less dangerous than coal dust, and the number of potash mines is significantly lower than the number of coal mines. However, the problem of dust content in potash mines is quite acute [5], and its solution cannot be carried out by transferring known methods from the coal industry. Traditional methods of dust suppression in coal mines, based on the use of water, are not applicable to the conditions present in potash mines. This is due to the lack of sufficient underground water: potash mines traditionally do not have underground plumbing systems. In the presence of hygroscopic salt rocks, waterlogging of rocks is unacceptable, as it leads to caking of salt particles and formation of an aggressive environment, which is dangerous and causes rapid corrosive wear on equipment. For this reason, it is necessary to explore other methods and approaches to dedusting the working areas of potash mines.

Salt dust has the following fundamental differences from coal dust: it is non-explosive and soluble in water [17]. The average particle size of potash dust at the mines of the Verkhnekamskoe and Starobinskoe salt deposits is 5–10 μm [5], while the average particle size of coal dust usually varies in the range of 50–150 μm [18,19]. This implies that the lifting of potash dust particles from the surfaces of mine workings and mining equipment by air flow begins earlier than for coal dust. For potash dust, the critical velocity is about 0.8–1 m/s [20], and for coal dust it is about 2 m/s [21]. This indicates that even ventilation solutions for dedusting coal mines cannot simply be transferred to potash mines.

This article examines the features of ventilation of dead-end drifts in potash mines with operating combines. Various auxiliary ventilation systems and air flow rates are considered. The article continues the previous studies of the authors [22,23]. In the first study [22], an approach was proposed that consists in dividing the air space of a dead-end drift into microzones and analyzing the airflows between this microzones. At the same time, it was proposed that the quality of the air in the "breathing zone" of miners be assessed by the quality of the air in the corresponding microzone, and not in the entire mine working. The possibility of using this approach is associated, first, with the distinctive property of potash dust, its lack of flammability. In [23], this approach was further developed. As a result of the analysis of mass transfer mechanisms in dead-end drift, it was shown that only when the convective mass transfer prevails over the diffusive one does it become possible to apply the microzoning approach. It is also shown that the convective mass transfer of air dominates only for the exhaust ventilation systems, while for forced ventilation systems, diffusive mass transfer prevails.

As in [20,23], our research methodology is based on multi-parameter numerical simulations of the flow of a dust–air mixture in a dead-end drift. However, in this article, greater attention is paid to the selection of adequate approaches to modeling dust aerosols, boundary conditions, parameterization, and validation of the model according to field experiments in potash mines.

While on the topic of methodology of numerical simulation, it is also important to note the existing methods and approaches to modeling the dynamics of dust aerosols in mines in general. Depending on the physical parameters of the medium (dispersion, concentration, and chemical activity), flow regimes, and geometry, dust aerosols are modeled as homogeneous multicomponent media [18,20,24] or as heterogeneous multiphase media [9]. Within

the latter framework, two approaches are distinguished: the Lagrange–Euler approach, wherein the dynamics of the dispersed phase (dust) are modeled by calculating the trajectories of individual particles [2,9,25] and the Euler–Euler approach, wherein the carrier phase (air) and the dispersed phase (gas) form two connected interpenetrating continua. In this case, separate transfer equations are considered for the dispersed phase [26]. Within the framework of the heterogeneous multiphase media model, the carrier and dispersed phases can have different velocities at each point of the continuum, while within the framework of the homogeneous multicomponent medium approach, the velocity field for all phases is common.

The more complex and complete Lagrange–Euler approach is applicable to essentially non-equilibrium flows (large inertial particles and rarefied dispersed media). It should be noted that this approach requires a large quantity of input data (the laws and parameters of the interactions between particles, as well as the particulate interaction with the air flow and the walls of mine workings) and is resource-intensive. The Euler–Euler approach is valid under conditions close to equilibrium (small, low-inertia particles, and concentrated dispersed media). The model of a homogeneous multicomponent medium is simplest and is used either when the components are mixed at the molecular level, or in a situation of a sufficiently low concentration of the dispersed phase (less than 0.1%) and small constituent particles (less than 10 μm). In the literature, the homogeneous medium model was used to study the distribution of gas impurities (methane) [27], to study the dynamics of the plume of diesel fuel particles created by a truck and loader [28], and to describe the dynamics of salt aerosols in the atmosphere [24,29].

Since the dust–air mixture by its nature is a two-phase medium (aerosol), in which the salt dust is present in the form of solid particles of small size and low volumetric concentration, it is most reasonable to use a simple model of a homogeneous multicomponent medium for numerical simulation. An additional motivation for choosing the simple modeling approach is that the parametrization of dust–air mixture models according to practical data is invariably difficult due to the small size of the datasets, their possible errors, and input data variability when considering different mine workings. At the same time, evaluation of the possibility of using simple models to describe the dynamics of a dust–air mixture should be made based on experimental studies of salt dust in relation to the object studied in this article, the atmosphere of a dead-end drift with an operating combine. Therefore, the plan of this study assumed, first, experimental measurements of air velocities and dust concentrations in a dead-end face, and second, the formulation of a mathematical model and its validation using numerical simulation data.

2. Experimental Studies of Dust Distribution in a Potash Mine

The measurements were carried out in the dead-end drift of the potash mine in the Verkhnekamskoye potassium-magnesium salt deposit (Russia, Perm Krai). The drift passes through the AB layer, which consists of two sublayers-in the lower part, sublayer A, represented by banded sylvinite, and in the upper part, sublayer B, represented by either carnallite or variegated sylvinite [30]. The length of the dead-end drift at the initial time (beginning of measurement procedure) was 150 m, and at the final time it was 157 m. The cross-sectional area of the drift was 15.6 m^2. Near the dead-end face, there was a Ural 20-R combine with a planetary executive body. A transfer bin was placed behind the combine (see Figure 1) and used for the accumulation of rock mass mined by the combine, and its subsequent reloading into a self-propelled car. The cross-section area of the drift was determined by the geometric features of the planetary executive body of the combine and is shown in Figure 2.

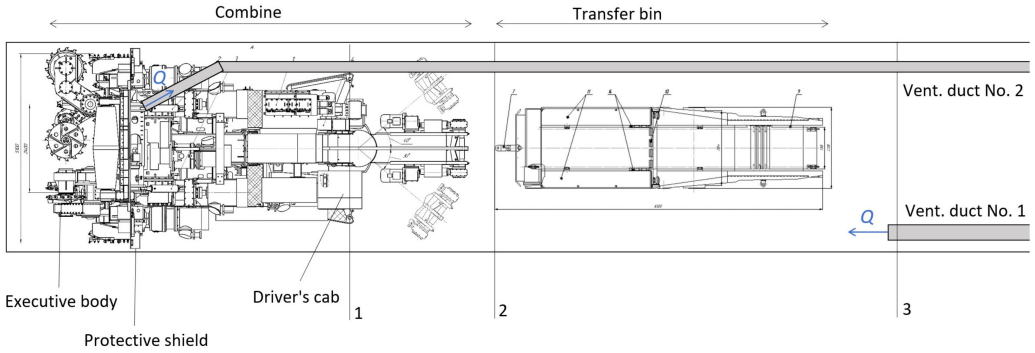

Figure 1. The position of the combine, transfer bin, and ventilation ducts in the dead-end drift (top view); measuring Sections 1, 2, and 3.

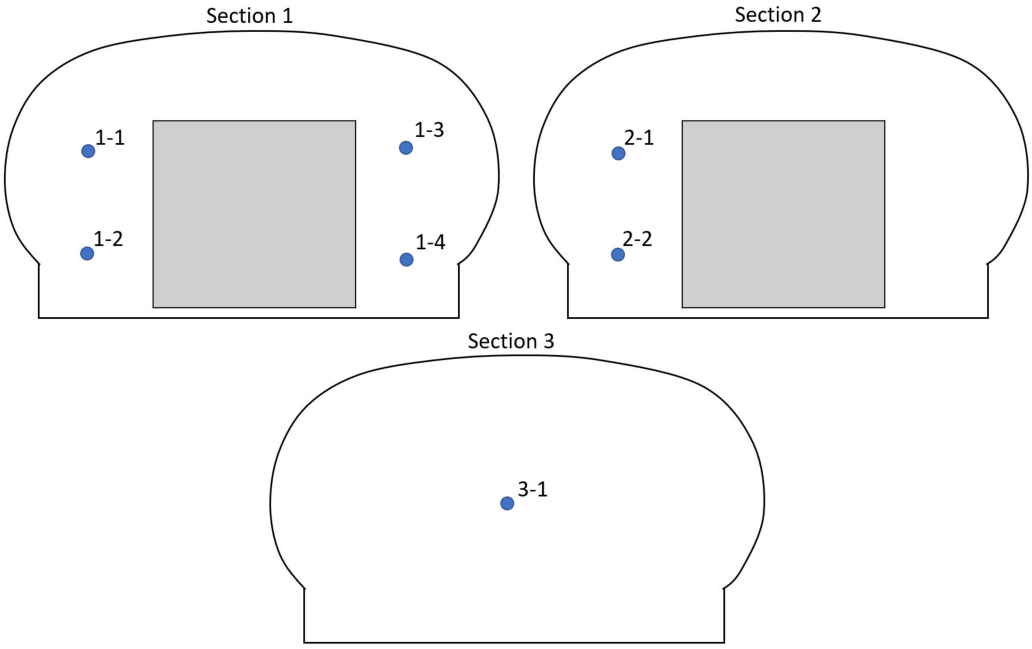

Figure 2. Dust measurement points for Sections 1, 2, and 3.

The main source of dust is an operating executive body that destroys the rock mass. The combine is equipped with a protective shield that prevents most of the dust from the executive body from entering the atmosphere of the drift. The protective shield is installed in the gaps between the combine and the drift walls along the perimeter of the drift. At the same time, some dust still penetrates the air space of the working through the cracks in the shield and the leaks between the shield and the wall of the dead-end drift. Another source of dust is the transfer bin, on which the mined ore is poured from the combine boom. These represent the primary two sources of dust.

Ventilation of the drift can be carried out using a forced ventilation system, an exhaust system, or their combination. In the case of a forced system, the stream of fresh air is supplied through the ventilation duct No. 1 (see Figure 1) and flows round the combine (up to the protective shield). The polluted air is removed through the drift. In the case of an exhaust ventilation system, fresh air is supplied to the combine through the drift, and the polluted air is removed through the ventilation duct No. 2. The combined system involves the use of both ventilation ducts and, in essence, is an intermediate option between the forced and exhaust systems.

The forced ventilation system is the most used system in the ventilation of dead-end faces. Most often, only the use of forced ventilation is permitted in mines. However, in addition to this system, in this study, we also considered the exhaust system. This

is because one of the practical issues of this study is to analyze the effectiveness of this ventilation system, in which convective mass transfer prevails over diffusion mixing and, in our opinion, it becomes possible to control the dust content of individual microzones.

Experimental studies were carried out for three cases of the ventilation of a dead-end face.

1. A forced ventilation system in which the distance between the end of the ventilation duct and the combine driver's cab is 10 m and the mean velocity of the air flowing out the ventilation duct is 19.4 m/s.
2. A forced ventilation system in which the distance between the end of the ventilation duct and the combine driver's cab is 25 m and the mean velocity of the air flowing out the ventilation duct is 20 m/s.
3. An exhaust ventilation system in which the air velocity at the inlet to the ventilation duct is 7.8 m/s. The air duct inlet is located on the combine, as shown in Figure 1.

For all three cases, the diameters of the ventilation ducts are identical (0.5 m). During the measurements, the combine was operating at full power. The time during which the operating combine moves 1 m (15–20 min) is quite large compared to the characteristic time of measuring air parameters in the section of the drift. Therefore, no corrections for the displacement of the measuring sections were made.

Figure 1 also shows the layout of the measurement sections in the longitudinal horizontal section of the drift. Figure 2 shows the measurement points for each measurement section. The combine driver's cab is located in Section 1 and corresponds to measuring points 1-1 and 1-2. At each point, a series of measurements of the dust concentration was carried out; the arithmetic mean was then calculated. A portable dust analyzer Testo CEL-712 Microdust Pro was used. The measurement range of dust mass concentration is 0.1–1500 mg/m^3 and the relative error is less than $\pm$10% (after a preliminary verification procedure). The air flow velocity at each point was measured using APR-2 anemometer with an absolute error equal to 0.03 + 0.02 $\times$ V(m/s). For each point, the velocity and mass concentration of dust were measured continuously for 0.5–1 min, after which the time-averaged value was calculated.

Table 1 shows the results of measurements of the mass concentration of dust for each case at measuring points located in Sections 1, 2, and 3. In general, we found that for all three cases, there are local zones in the dead-end drift with a high dust concentration of more than 90 mg/m^3 (mainly in Section 1). On average, the concentrations for all three cases are comparable (for the second case, the concentrations are slightly higher). The standard deviations of the dust concentrations for each case are also comparable. The results do not allow us to conclude that one ventilation system or another is superior solely based on experimental measurements. At the same time, it is important to note that the air flow rate in case 3 is 2.5 times lower than for cases 1 and 2.

Table 1. Measured dust concentrations.

Measuring Point	Dust Concentration, mg/m^3		
	Case 1	Case 2	Case 3
1–1	27.5	57.3	99.5
1–2	46.6	108.2	32.9
1–3	88.8	109.8	92.9
1–4	94.5	108.2	46.7
2–1	66.6	52.8	54.0
2–2	53.2	93.2	29.3
3–1	69.0	32.6	32.2
Mean value	63.7	80.3	55.3
Standard deviation	23.5	32.0	29.3

At the measuring points corresponding to the combine driver's cab, the lowest dust concentrations were measured for the first and third cases. This is explained by the

following facts: In the first case, there is intense mass transfer around the cab due to the influence of a stream of fresh air coming out of the ventilation duct. The measured local air velocity in this zone for case 1 is 2–2.5 m/s. As a result, the dust is diluted in a sufficiently large volume of air, and its concentration drops. In the third case, the dust source closest to the driver's cab (transfer bin) does not have time to significantly affect the air quality in the cab zone, since convective mass transfer dominates and is directed towards the ventilation duct on the right side of the combine. When operating with the concepts "right side" and "left side" of the combine, it is assumed that the observer is at the mouth of a dead-end drift-in this case, the driver's cab for the observer is to the left of the combine.

At the same time, the air velocity near the driver's cab for the third case is significantly lower than for cases 1 and 2 and varies in the range of 0.17–0.37 m/s. Thus, the relatively low air velocity provides more comfortable working conditions.

The maximum measured dust concentration was about 110 mg/m^3, which corresponds to a dust volume concentration of less than 0.00001%. At the same time, local dust concentrations near the combine shield and transfer bin will be significantly higher; however, in general, it can be concluded that for most of the air space of a mine working, the thesis that the volume concentration of dust does not exceed 0.1% is correct. Considering that the average size of dust particles for the Verkhnekamskoye deposit does not exceed 10 μm [5], it is appropriate to use the single-velocity continuum approach to model the distribution of dust in a dead-end drift, since the dust does not significantly affect the dynamics of air flows in a dead-end drift, and the interaction between individual dust particles is insignificant. In this sense, the dust aerosol behaves like a homogeneous multicomponent mixture (while not being one in essence).

The minimum measured dust concentration is about 30 mg/m^3. This is true even for the exhaust ventilation, although for it at point 3-1 the air must be clean. However, under real conditions, the ventilation duct through which dusty air is removed is rarely completely sealed. It consists of separately interconnected elements through which a small amount of dusty air enters the atmosphere of the drift. The resulting background concentration of dust (about 30 mg/m^3) characterizes the tightness of the ventilation duct.

This section does not contain analysis of the airflow distribution within the considered cases, since this analysis is conducted in the following sections of the article during model validation.

3. Mathematical Model and Its Numerical Implementation

At the next stage of the study, we formulated a mathematical model that describes the spread of dust in a dead-end drift during the operation of a combine. The main assumptions are presented below:

1. The dust particles do not affect the air flow and move along with it (the dust aerosol is a one-velocity continuum);
2. The dust particles are of the same size and do not interact with each other, and do not absorb moisture from the air;
3. The dust–air mixture behaves like an incompressible medium;
4. The density of dust–air mixture depends on temperature;
5. There exists a local thermodynamic equilibrium between phases;
6. The distribution of all parameters of the dust–air mixture is stationary;
7. Gravitational settling and coagulation of dust particles are not considered.

Assumption 7 is possible due to the high velocities of the air in the dead-end drift and its relatively small length. The characteristic times of gravitational settling and coagulation of dust particles turn out to be significantly higher than the characteristic time of dust particle presence in the considered section of the mine until it enters the ventilation duct or leaves the part of the drift under consideration.

The model is based on the mass, momentum, and energy balance equations in the steady-state formulation written for the mixture as a whole:

$$\nabla \cdot \vec{V} = 0 \tag{1}$$

$$\rho \vec{V} \cdot \nabla \vec{V} = -\nabla p + \nabla \cdot \left[(\mu + \mu_t) \nabla \vec{V} \right] + \rho \vec{g} \tag{2}$$

$$\nabla \cdot \left[\vec{V} (\rho e + p) \right] = \nabla \cdot [(\lambda + \lambda_t) \nabla T] \tag{3}$$

where $\vec{V}$ is the velocity vector of the dust–air mixture in m/s, p is the pressure in Pa, μ and μ_t are molecular and turbulent viscosities in Pa·s, ρ is the density of the dust–air mixture in kg/m^3, $\vec{g}$ is the gravity vector in m/s^2, e is the specific internal energy of the dust–air mixture in J/kg, λ and λ_t are molecular and turbulent thermal conductivities in W/(m·°C), and T is the temperature in °C.

The specific internal energy of the dust–air mixture depends on the temperature according to the following relation:

$$e = c_p T - \frac{p}{\rho} + \frac{V^2}{2} \tag{4}$$

where V is the velocity magnitude of the dust–air mixture in m/s and c_p is the specific heat capacity of the dust–air mixture in J/(kg·°C).

The system is supplemented by the ideal-gas equation of state:

$$p = \rho R \tag{5}$$

where R is the individual gas constant for air in J/(kg·°C).

Turbulent viscosity and thermal conductivity are determined based on the characteristics of the turbulent flow—in this case, the turbulent kinetic energy k and the dissipation rate of the turbulent kinetic energy, ε [31]:

$$\mu_t = \frac{\rho C_\mu k^2}{\varepsilon} \tag{6}$$

$$\lambda_t = \mu_t \frac{c_p}{\mathrm{Pr}_t} \quad \mathrm{Pr}_t = 0.85, \tag{7}$$

where C_μ is the model constant and Pr_t is the turbulent Prandtl number.

The realizable k-ε turbulence model [32] is used to close the above system of equations. The C_μ parameter in Equation (6) is calculated using the formula:

$$C_\mu = \frac{1}{4.04 + \sqrt{6} cos\phi \frac{k\sqrt{\overline{\overline{S}} \cdot \overline{\overline{S}} + \widetilde{\Omega} \cdot \widetilde{\Omega}}}{\varepsilon}}, \tag{8}$$

$$\phi = \frac{1}{3} \cos^{-1}\left(\sqrt{6} W\right) \quad W = \frac{\overline{\overline{S}} \cdot \left(\overline{\overline{S}} \cdot \overline{\overline{S}}\right)^T}{\left(\overline{\overline{S}} \cdot \overline{\overline{S}}\right)^{3/2}} \quad \overline{\overline{S}} = \frac{1}{2}\left[\nabla \vec{V} + \left(\nabla \vec{V}\right)^T\right] \tag{9}$$

$$\widetilde{\Omega} = \overline{\overline{\Omega}} - 2\overline{\overline{E}} \cdot \vec{\omega} \tag{10}$$

where $\overline{\overline{S}}$ is the symmetric part of the strain rate tensor in 1/s, $\overline{\overline{\Omega}}$ is the asymmetric part of the strain rate tensor in 1/s, $\overline{\overline{E}}$ is the Levi-Civita tensor, $\vec{\omega}$ is the vector of the angular velocity of the dust–air mixture in 1/s, and ϕ and W are the model parameters.

In accordance with the realizable k-ε model, the evolution of turbulent kinetic energy and dissipation rate are described by the equations:

$$\rho\left[\frac{\partial k}{\partial t}+\nabla\cdot\left(k\vec{V}\right)\right]=\nabla\cdot\left[\left(\mu+\frac{\mu_t}{\sigma_k}\right)\nabla k\right]+P_k+P_b-\rho\varepsilon+S_k \tag{11}$$

$$\rho\left[\frac{\partial \varepsilon}{\partial t}+\nabla\cdot\left(\varepsilon\vec{V}\right)\right]=\nabla\cdot\left[\left(\mu+\frac{\mu_t}{\sigma_\varepsilon}\right)\nabla \varepsilon\right]+\rho C_1 S\varepsilon-\rho C_2\frac{\varepsilon^2}{k+\sqrt{\nu\varepsilon}}+C_{1\varepsilon}\frac{\varepsilon}{k}C_{3\varepsilon}P_b \tag{12}$$

$$C_1=\max\left[0.43,\frac{\eta}{\eta+5}\right]\ \ \eta=S\frac{k}{\varepsilon}\ \ S=\sqrt{2\overline{\overline{S}}\cdot\cdot\overline{\overline{S}}} \tag{13}$$

where P_k, P_b, and S_k are the terms that characterize the generation of turbulent kinetic energy measured in kg/(m·s^3) and C_1 and η are the model parameters.

The model constants are as follows:

$$C_{1\varepsilon}=1.44\ \ C_2=1.9\ \ \sigma_k=1.0\ \ \sigma_\varepsilon=1.2 \tag{14}$$

The Menter-Lechner model [33] was used to describe the flow behavior in a thin boundary layer near the solid walls. The essence of this model is the source term S_k in the turbulent kinetic energy equation, which accounts for near-wall effects. The additional term S_k is non-zero only in a viscous sublayer near the solid walls. In the logarithmic region, it automatically becomes zero.

Combine engines are equipped with cooling systems (small fans), through which air is forced to flow at a certain rate. To take this factor into account in the model, a condition was set on the internal surfaces of the five engines of the combine in the form of a fixed tangential velocity component (see Figure 3a). In most calculations, the tangential velocity component is assumed to be 5 m/s. This made it possible to obtain air flow through the engine comparable to the real one. The value of the tangential velocity was determined based on experimental measurements of air circulation in the engines.

At the outflow of the ventilation duct, the air velocity was fixed. The air velocity value is positive with the forced ventilation system and negative with the exhaust ventilation system. The static pressure was set to zero at the mouth of the dead-end drift.

The temperature of the drift walls was assumed to be 10 °C. At the same time, the temperature of the internal surfaces of the combine engines is 50 °C, which was also selected based on experimental studies of the temperature of the air leaving the engines during the operation of the combine. On the walls of the combine, a condition of no heat flow was imposed. The temperature of the air entering the computational domain was assumed to be 10 °C.

The dynamics of the salt dust were described using a simple convection-diffusion model of passive impurity. In this case, due to the low concentration of dust over the course of the numerical simulation, it was convenient to introduce a dimensionless concentration C. The value of the dust concentration near contaminated surfaces is taken as a unit of measurement of the concentration C, i.e., the maximum concentration of dust in the drift, while the zero value of the dimensionless concentration corresponds to the background level of dust content at the drift's mouth. The distribution of dust is determined from the transport equation:

$$\frac{\partial C}{\partial t}+\vec{V}\cdot\nabla C=\nabla\cdot[(D+D_t)\nabla C] \tag{15}$$

where D is the diffusion coefficient measured in m/s^2, adjusted according to the experimental data and D_t is the coefficient of turbulent diffusion in m/s^2, calculated as the ratio of the turbulent viscosity and the turbulent Schmidt number for air.

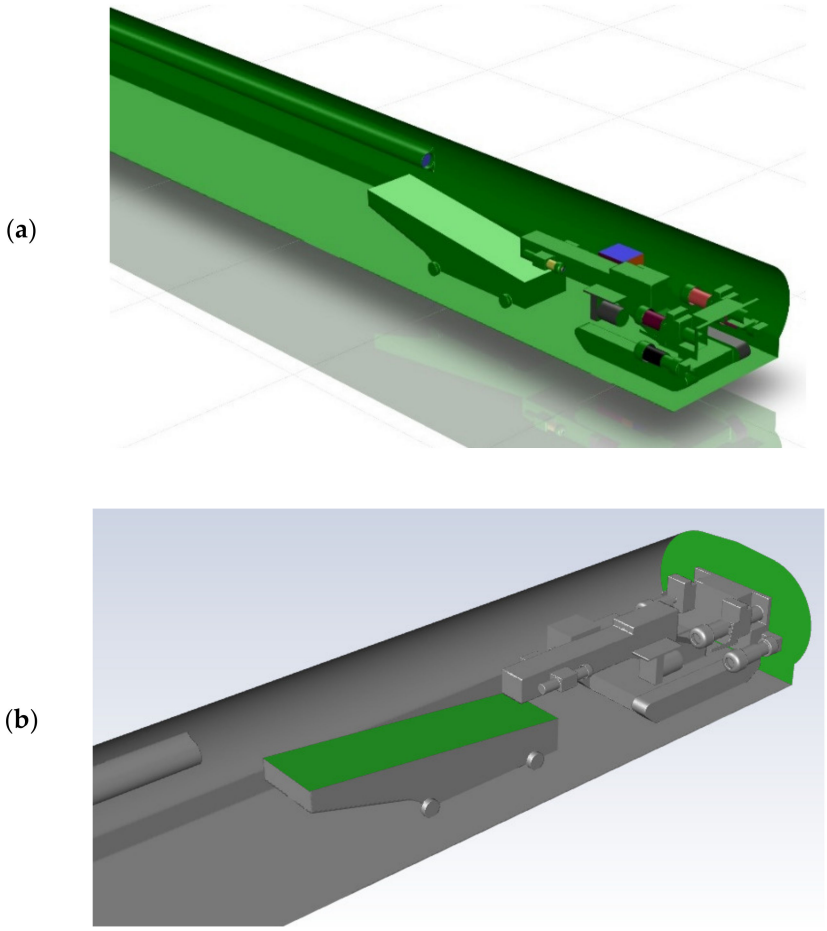

Figure 3. The geometry of the computational domain: (**a**) The combine engines (cylinders) and the driver's cab (rectangular block) are highlighted in color. (**b**) The surfaces where dust is generated are highlighted in color.

As noted above, the process of dust formation is observed mainly near the combine protective shield and the upper part of the transfer bin. In this regard, the proposed model considers two surface sources of dust. The first is located on the surface of the combine protective shield, the second on the upper surface of the transfer bin (see Figure 3b). On these surfaces, the boundary condition (in terms of the dimensionless concentration) $C = 1$ was set. At that, the space behind the protective shield, where the executive body operates, is not considered in the model.

It is important to note that the chosen source boundary condition is atypical for the study of dust aerosol dynamics in mines. In works related to the modeling of coal dust in longwalls, a constant dust flow boundary condition is most often used [34]. This is reasonable if the dust inflow from the object generating this dust is modeled explicitly, or the experimental data are used. In our case, the dust generation surfaces are effective surfaces; that is, dust generation does not occur directly on them. For example, in the case of a transfer bin, because of crushed ore from the combine boom falling into the hold of the transfer bin, a dust cloud is formed above the hold, partially limited by the walls of the hold. In this case, there is both a constant influx of dust mass to the dust cloud, and a constant outflow due to local settling of dust back into the hold, as well as due to convective transfer of dust by the air flowing through the dust cloud. In this case, it is assumed that approximately the same concentration of dust is maintained in the steady dust cloud. As such, under the chosen effective dust formation surface in Figure 3b, one can understand the conventional boundary of this dust cloud. This assumption is valid when the intensity of convective dust transfer from the cloud is lower than the intensity of

dust release as a result of falling crushed ore. At the same time, an increase in the air flow passing through this source of dust formation leads to increase in the dust captured and transferred by the air.

It was assumed that dust settles on the drift walls. For this reason, the boundary condition $C = 0$ was set on the walls. In contrast to the working surface, a combine is in high-dust conditions for a long time and its surface is usually covered with a significant layer of dust. Therefore, it is more difficult for dust particles to cling to the surface of the combine. In addition, the walls of the combine usually have a relatively low roughness and are subject to vibrations during its operation. To consider the described effects on the combine walls, the boundary condition $\partial C/\partial n = 0$ was set, where n is the normal vector to the boundary. This corresponds to the case in which the processes of settling and escape of dust particles from the wall occur with the same intensity and, thus, compensate each other.

It is important to note that the model does not consider the processes of coagulation and condensation of salt aerosol particles in the interior points of the domain. These physical processes can be significant if we consider a sufficiently long movement of salt aerosol along sufficiently long tracts under conditions of high relative humidity of the flow [35]. In the present work, a relatively short domain is considered. The characteristic time for a dust particle to pass through this drift is rather short, and the relative air humidity is low (about 30%, according to the experimental data), so that the particles do not absorb moisture and do not have time to coagulate.

The dimensional concentration of dust was calculated by the formula:

$$C_p = C_0 + \frac{r}{\overline{C}} C \tag{16}$$

where C_0 is the dust concentration in the drift far from dust sources (background level) in mg/m^3, $\overline{C}$ is the average dimensionless dust concentration calculated during the simulation, and r is the model parameter that has the dimension of dust concentration and is adjusted on the basis of the available experimental data on the dust concentrations, measured in mg/m^3.

The average dimensionless concentration $\overline{C}$ was calculated over the course of the simulation from the average dust concentration at the boundary through which the air leaves the computational domain. In case of an exhaust ventilation system, this is the ventilation duct, and in the case of forced ventilation system, it is the drift's mouth.

The computational domain was a dead-end drift 50 m long. The vertical section of the drift is shown in Figures 2 and 3. Numerical simulation was carried out for a simplified model of a combine, which incorporated all the large elements that affect the dynamics of air and dust (see Figure 3). The subsequent detailing of the model leads to an exponential increase in the finite volume count in the computational mesh and to worsening of the convergence of the solution. This is related to the appearance of complex connections between individual parts of the combine and thin flow areas between them.

At the first stage of creating the computational mesh, a hexagonal two-dimensional mesh was generated at all boundaries of the computational domain. Then, a three-dimensional mesh was built considering the boundary layer near solid surfaces. The volume mesh consisted of polyhedra (see Figure 4). The choice of this type of element is due to a significant reduction in the number of finite volumes compared to a tetrahedral mesh. As a result, the solution convergence becomes faster and the amount of memory required for the calculation is reduced. In the case of the forced ventilation system, the computational mesh consists of 4.6 million nodes and 1.2 million finite volumes (or cells).

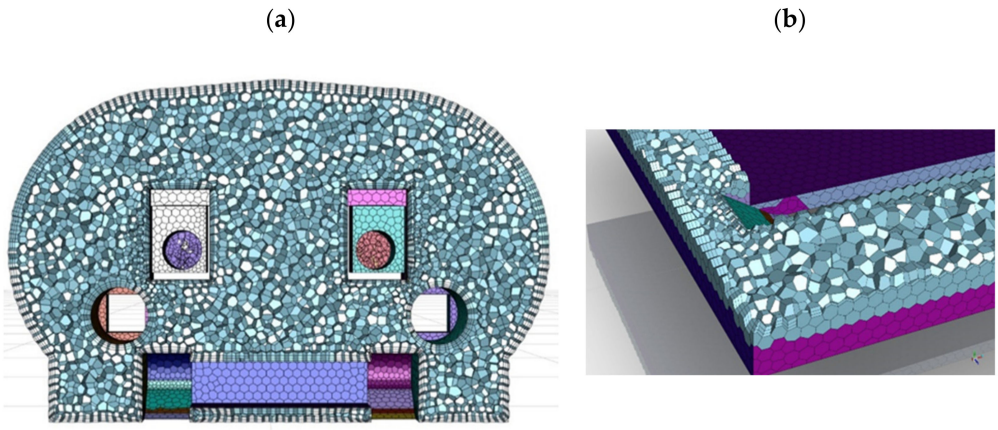

Figure 4. Computational mesh at (**a**) vertical cross-section of the combine and (**b**) near the mine wall.

The spatial discretization of the equations was carried out using Monotonic Upstream-centered Scheme for Conservation Laws (MUSCL) scheme that was third-order in accuracy [36]. The method of pseudo-evolutionary equations was used. While solving the stationary problem, iterations were carried out over the effective time until the stationary solution was reached.

4. Model Parametrization

The model parametrization was conducted based on the measured geometric dimensions of the dead-end drift, ventilation ducts, combine, and transfer bin, as well as the measured aerodynamic parameters (air velocity in the duct and background dust concentrations). There are also two parameters (D and r) in the model, the values of which were adjusted to produce the best agreement between the calculations and field measurements for all three ventilation cases described in the Section 2 of this article. As a result of the model parametrization procedure, we obtained the following values: $D = 5{\cdot}10^{-5}$ m^2/s; $r = 28$ mg/m^3.

It is important to note that both adjustable parameters refer to the dust concentration field in a dead-end drift, while to improve the correspondence between the calculated and measured velocity fields, such parameters were not used. We tried to match the calculated velocity field and experimental velocity measurements by choosing the geometric parameters of the model that most reliably reflect the real geometry of the combine, drift, and ventilation duct. At the same time, several factors (some details of the geometry of the combine, the transfer bin, the unevenness of the drift walls and ventilation ducts, et cetera) remained unaccounted for in the model. This led to the impossibility of obtaining a perfect match between the measured and calculated aerodynamic parameters of the air for all measured sections and ventilation options. Figures 5 and 6 show the model and experimental dependences of dimensional dust concentration and air velocity on the vertical coordinate, carried out in measurements along the selected vertical lines to the right and left of the combine in several cross sections of the dead-end drift.

The blue dots in Figures 5 and 6 correspond to experimental measurement data, and the dotted lines between them correspond to the piecewise linear approximations. The profiles of velocity and dust concentrations in all considered sections have a rather complex non-linear and non-monotonic character both along the vertical coordinate and along the horizontal axis of the drift. This indicates the complex structure of the flows that form in the vicinity of the combine and the transfer bin. Thus, the measurement result may be sensitive to some small variations in the geometry of the combine and the position of the measurement points. The experimental points, in addition to the error of the instruments, also have a small error associated with determining the vertical coordinate of each point ($\pm$5 cm).

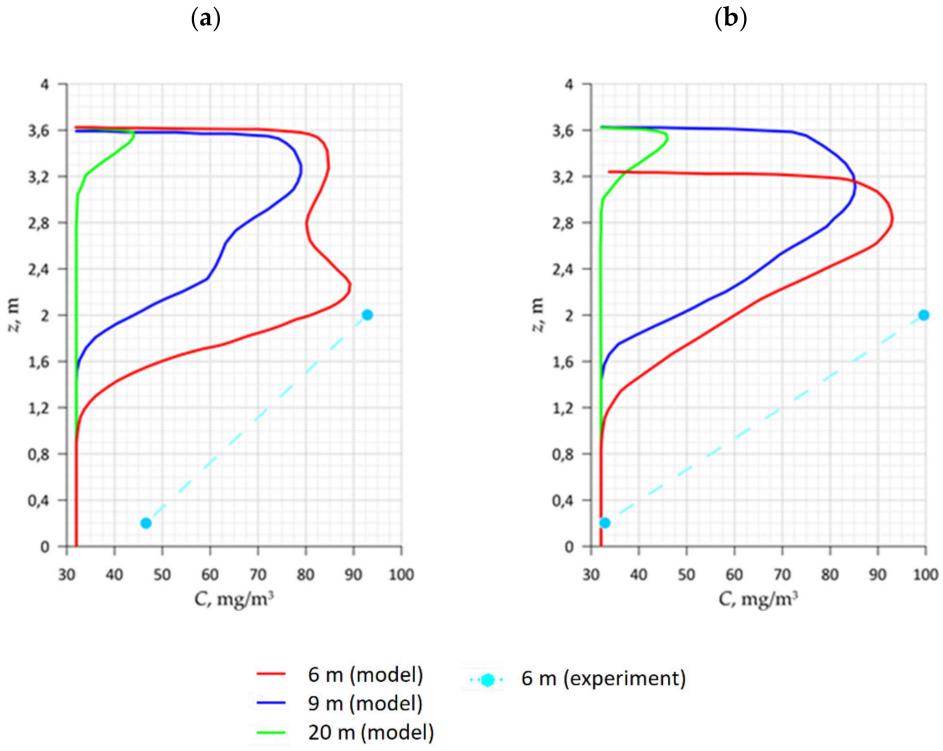

Figure 5. Comparative analysis of the distribution of dimensional dust concentration along the vertical lines of Section 2 to the right (**a**) and to the left (**b**) of the combine, exhaust ventilation system.

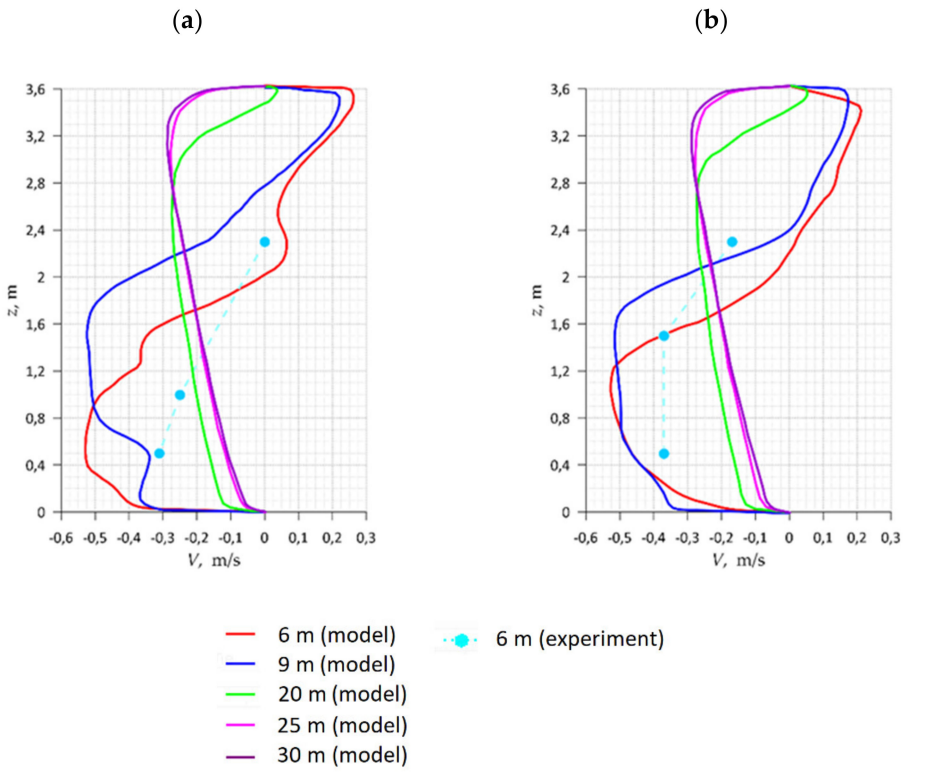

Figure 6. Comparative analysis of the distribution of the air flow velocity along the vertical lines of Section 2 to the right (**a**) and to the left (**b**) of the combine, exhaust ventilation system.

The figures show that while quantitatively the results sometimes differ greatly, in all cases, the theoretical and experimental curves show a similar qualitative behavior. For this reason, in the final validation of the model, we were primarily guided by the presence

of a qualitative correspondence between the simulation data and the data of a full-scale experiment for all considered cases. At the same time, the conclusions obtained using this model should be considered precisely at the qualitative level without relying on the specific quantitative characteristics of the dust–air mixture.

5. Discussion

5.1. Forced Ventilation System

The described model was used to conduct several numerical simulations with various options for the ventilation of a dead-end drift. First, the influence of various air flows through the drift on the dust concentration field is considered. Figure 7 shows the streamlines in the dust–air mixture in the domain with a forced ventilation. The distance between the driver's cab and the ventilation duct is 10 m, and the duct itself is located near the drift's bottom to the left of the combine. The velocity of the air leaving the ventilation duct is 19.4 m/s and the diameter of the ventilation duct is 0.5 m. Thus, the amount of air supplied to the working area face was 3.8 m^3/s.

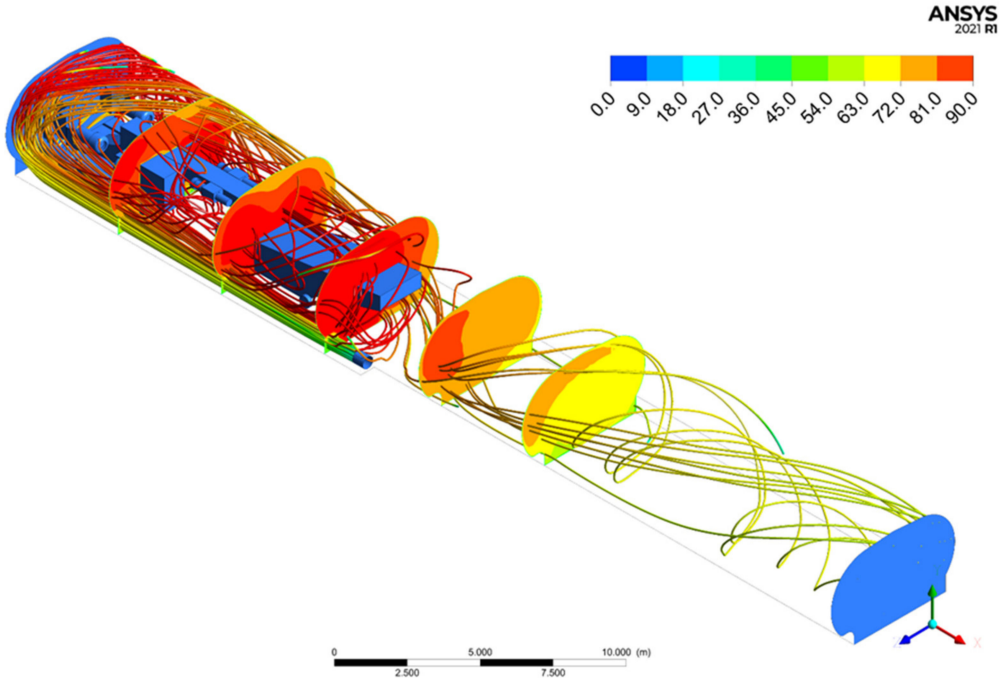

Figure 7. Calculated streamlines in a drift with forced ventilation system (Q = 3.8 m^3/s). The color shows the concentration of dust in the domain.

Figure 7 shows that the air emerging from the ventilation duct moves towards the face and the combine driver's cab. At the same time, the local zone near the combine driver is quite dusty, due the formation of a large vortex in the drift when a forced ventilation system is used. A stream of high-velocity fresh air moves towards the bottom from the left side of the combine, picks up dust on the protective shield, and moves in the opposite direction, mainly from the left side of the combine. A fraction of the air, flowing around the transfer bin and picking up the dust released in the process of pouring ore into the bin, returns to the protective shield passing through the combine driver's cab.

The presence of a vortex seriously worsens the dust situation in the driver's cab zone. It should also be noted that under the conditions of the Verkhnekamskoye potash salt deposit, the air temperature in excavations is on average 10–12 °C, and the air velocity in the driver's cab in the drift is 2–2.5 m/s, as mentioned earlier. This creates uncomfortable microclimate conditions for miners, which is another negative aspect of the forced ventilation system.

The simulation results for other air flows in the drift showed that the vortex, which is shown for the standard ventilation parameters on Figure 7, is present both with a two-times decreased air flow and two-times increased air flow.

An analysis of changes in the dust concentration near the combine driver's cab was carried out, depending on the air flow in the drift. The dust concentration profiles along several vertical lines passing at a distance of 9, 20, and 25 m from the combine shield are shown in Figure 8. The distance of 9 m from the shield of the combine corresponds to the driver's cab.

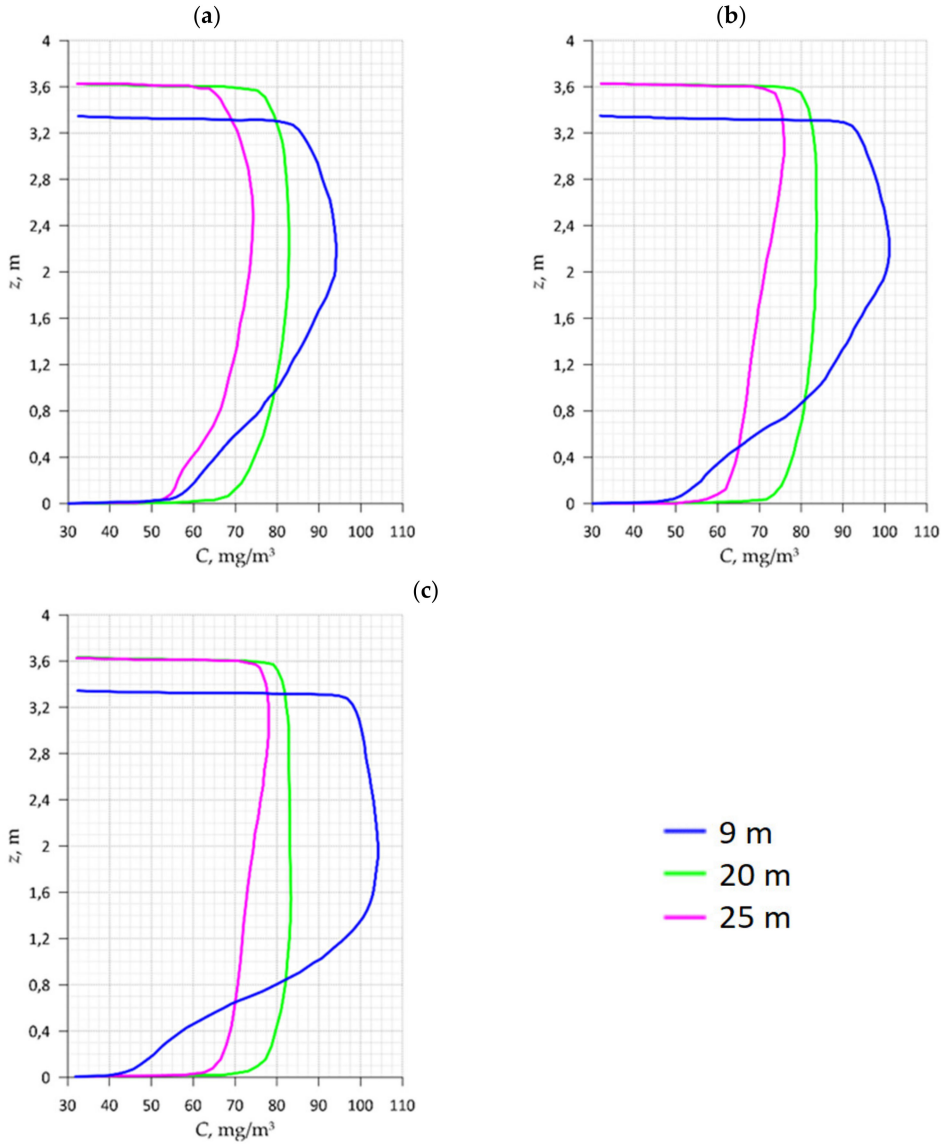

Figure 8. Dimensional dust concentration at the measuring point near the combine for different air flow rates: (**a**) 1.9 m^3/s, (**b**) 3.8 m^3/s, (**c**) 7.6 m^3/s, forced ventilation system.

Figure 8 shows that a two-times increase in the air flow does not lead to a decrease in the dust concentration in the breathing zone of the combine driver. Moreover, the results of the numerical simulation indicate a certain increase in the mass concentration of dust at a height of 1.5 to 2 m around the driver's cab. At the same time, with a decrease in the air flow, the mass concentration of dust in the zone of the combine driver's cab decreases.

The higher the air flow during the forced ventilation method, the higher the intensity of the vortex passing through the transfer bin and, as a result, the higher the amount of dust picked up by the air vortex and brought to the workplace of the combine driver. On the other hand, the higher the air flow, the more air dilutes the dust picked up from two considered sources of dust. In general, these factors should compensate each other. This follows from the fact that at 25 m from the combine shield and the transfer bin, where the air

velocity along the drift cross section is equalized, the dust concentration is approximately identical (72–75 mg/m^3) for any of the three air flow rates considered. At the same time, for certain local zones of dead-end drift, compensation may not occur; that is, one factor may dominate over the other. This is precisely what happens for the area near the combine driver's cab—the second factor turns out to be slightly weaker than the first, which leads to an increase in concentration with an increase in air flow.

At first glance, it may seem that it is possible to minimize the concentration of dust in the breathing zone of a combine driver by determining the optimal (and rather low) air flow. This statement would be true if the extraction of potash ore did not emit other hazardous substances, such as combustible and toxic gases. However, the emission of methane and hydrogen sulfide can occur in potash mines in various situations. Furthermore, taking into account the smallness of the optimal air flow in terms of the dust factor (less than 1.9 m^3/s), this value may not be enough to dilute gases to safe concentrations. In this regard, it is necessary to consider other ways to normalize the dust situation in dead-end drifts in potash mines. For this purpose, the results of numerical experiments using the exhaust ventilation system are considered below.

5.2. Exhaust Ventilation System

Each combine (from the Ural brand) is equipped with a dust collection system consisting of an intake fan and a fabric filter. This system is extremely inefficient, since the fabric filter becomes clogged with dust in a very short period. The idea of the numerical experiment was to evaluate the efficiency of the exhaust ventilation system, using a standard intake fan as a draft source. The fan exhaust is connected to the inflow of ventilation duct No. 2, through which dusty air is removed from the dead-end drift. Technically, this option is very convenient because its implementation will not require significant costs.

Next, we carried out a series of numerical calculations of the model of a dead-end drift with an exhaust ventilation system at different air flow rates in ventilation duct No. 2: under standard conditions (provided by a regular intake fan), air flow was 3.12 m^3/s (Figure 9b), with the air flow increased by 1.5 times, the air flow was 4.68 m^3/s (Figure 9c), and with the air flow decreased by 1.5 times, the air flow was 2.08 m^3/s (Figure 9a).

The simulation results for the standard ventilation mode (Figure 9b) show that in the case of exhaust ventilation, the dust concentration increases with height. On the left side of the combine (near the combine driver's cab) at a height of 2 m, the dust concentration is 48–60 mg/m^3 (zone 6–9 m from the shield), and at a height of 3 m, it is already around 85 mg/m^3 to 92 mg/m^3. This conclusion is confirmed by the visualization of the streamlines of the dust–air mixture (Figure 10b).

The results of a numerical experiment for reduced air flow (Figure 9a) show that with a decrease in air flow, an increase in dust concentration occurs at a height of 2 m. Quantitatively, the mass concentration of dust did not increase substantially; however, it is important to conclude that in qualitative terms, for the exhaust ventilation we see, that a decrease in air flow in the drift leads to an increase in dust concentration.

In turn, an increase in the performance of the intake fan (Figure 9c) makes it possible to reduce the dust concentration at 6 to 9 m from the combine shield (driver's cab zone) to 32–52 mg/m^3. It should be noted that the value of 32 mg/m^3 is the background dust concentration, and that in the absence of air leaks from the ventilation dust, the background concentration will be close to the permissible values, around 5 mg/m^3. The concentration of dust at 6–9 m from the shield at a given air flow rate will also be the same.

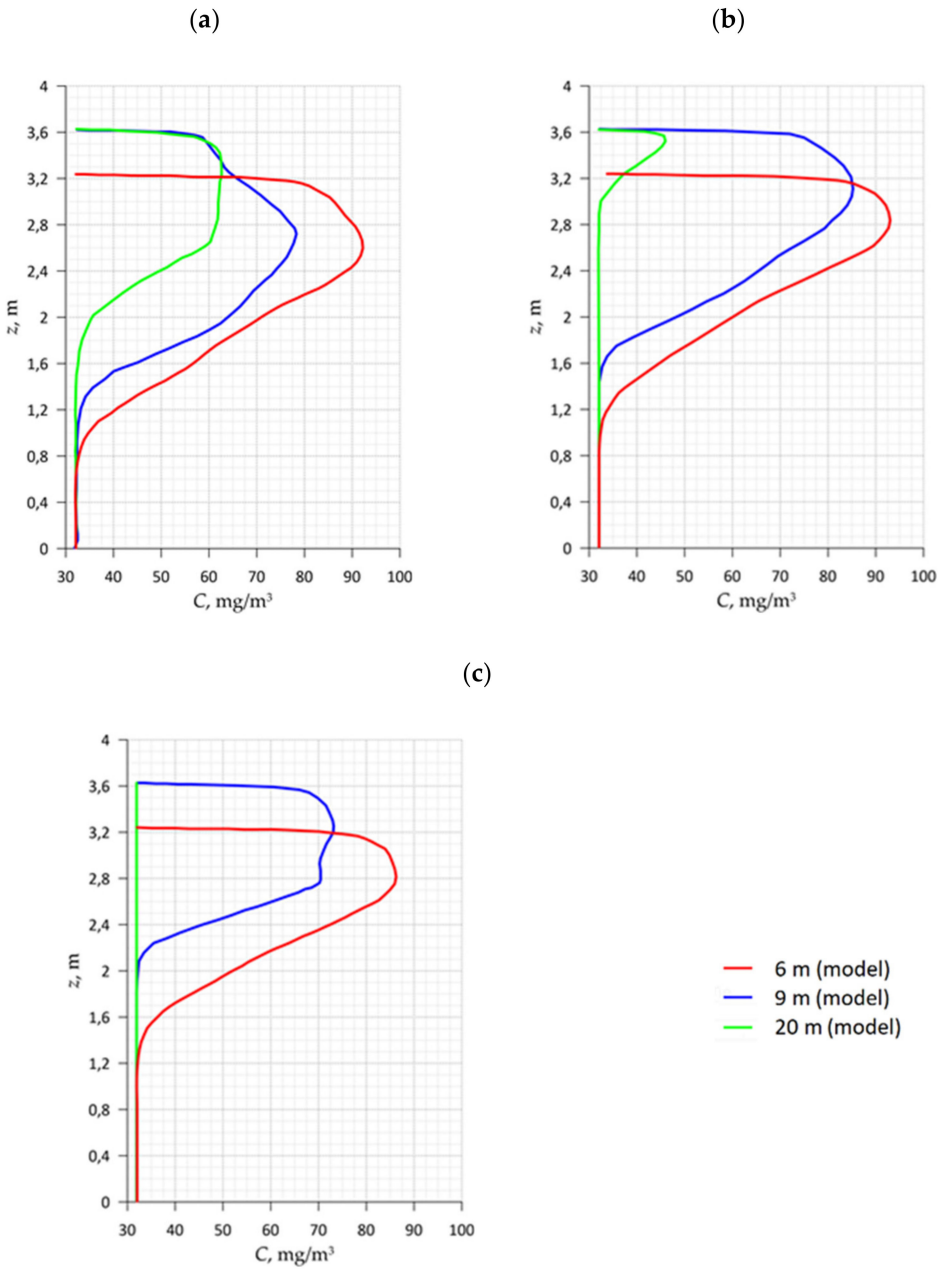

Figure 9. Mass concentration of dust at the measuring point near the combine for different air flow rates: (**a**) 2.08 m^3/s, (**b**) 3.12 m^3/s, (**c**) 4.68 m^3/s, exhaust ventilation system.

The decrease in dust concentration with an increase in air flow can be physically interpreted as follows: the higher the air flow in a drift, the closer the dust cloud can be shifted to the dead-end face and to the roof of the drift. It is obvious that the section of the drift in which the intake fan (and ventilation duct entry) is located is the boundary beyond which it is impossible to move the dust cloud. As mentioned above, the combine driver's cab and the intake fan are in the same section. Moving the fan intake point as close as possible to the protective shield will allow one to localize the dust cloud in the smaller part of the drift, and the driver's cab will be in a minimally dusty atmosphere. This thesis follows from the results of numerical simulations carried out for the case of a fan displaced towards the shield (Figure 10) for standard ventilation conditions.

It can be noted that moving the fan to the shield makes it possible to localize dust flows mainly on the right side of the combine (opposite from the driver's cab) in the immediate vicinity of the shield. Dust content is partially fixed in the sections located up to the driver's

cab, which is natural since the transfer bin, like the combine, is a dust generator. However, it should be noted that the dust generated during the pouring of ore into the transfer bin is shifted to the right side of the working, opposite the driver's cab, since the intake fan and the entry of the ventilation duct are located on the right.

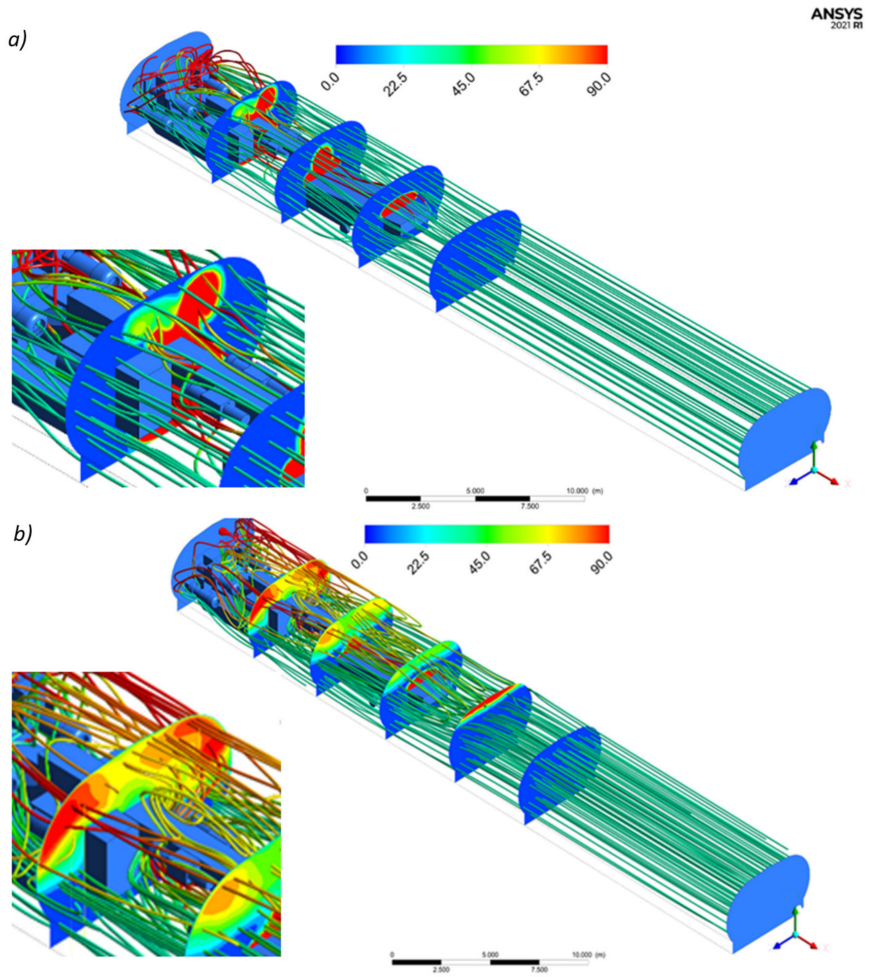

Figure 10. Dust–air mixture streamlines for exhaust ventilation at different intake fan positions: (**a**) 0.5 m from the protective shield, (**b**) opposite the combine driver's cab. The color shows the dimensional concentration of dust.

Comparing the quantitative values of the mass concentration of dust in the area where the combine driver is located, it can be noted that when the intake fan is shifted to the protective shield, the dust concentration corresponds to the background values used in the calculation. At the same time, to the right of the combine (at the cabin level), the concentration also corresponds to the background concentration. The dust generated during the pouring of ore into the transfer bin is mainly localized in the upper central part with a subsequent rightward shift.

6. Conclusions

The article deals with the issue of controlling the dust content of dead-end drifts in potash mines. A mathematical model of a dust–air mixture dynamics in a dead-end drift with operating combine is proposed. The model is also parametrized according to the data of experimental studies in a potash mine of the Verkhnekamskoye potassium-magnesium salt deposit. As a result of multi-parameter simulations carried out with the model, the following main results were obtained:

1. The forced ventilation system leads to the formation of a stable large-scale vortex in the drift. The vortex characteristically returns a portion of the dusty air flows back to the combine driver's cab in a wide range of the air flows. An increase in the air flow leads to an increase in dust concentrations at the location of the combine driver.
2. The exhaust ventilation system permits the localization of the dust cloud near the dead-end face, and thereby, reduces the concentration of dust in a part of the drift, including the zone where the combine driver is located. The degree of localization can be controlled by changing the performance of the intake fan. With an increase in the air flow rate, the degree of dust localization also increases.
3. Moving the intake fan as close as possible to the protective shield allows one to localize the dust cloud in the immediate vicinity of the shield, ensuring that the combine driver's cab will be in an atmosphere with the minimum dust concentration.

Author Contributions: Conceptualization, L.L. and A.I. (Aleksey Isaevich); methodology, A.I. (Aleksey Isaevich) and M.S.; software, A.I. (Andrey Ivantsov); validation, A.I. (Aleksey Isaevich), M.S. and A.I. (Andrey Ivantsov); formal analysis, A.I. (Andrey Ivantsov) and M.S.; investigation, A.I. (Andrey Ivantsov); resources, A.I. (Aleksey Isaevich); data curation, T.L. and L.L.; writing—original draft preparation, A.I. (Aleksey Isaevich) and M.S.; writing—review and editing, T.L. and A.I. (Andrey Ivantsov); visualization, A.I. (Andrey Ivantsov); supervision, L.L.; project administration, L.L; funding acquisition, L.L, A.I. (Aleksey Isaevich), M.S. and A.I. (Andrey Ivantsov) All authors have read and agreed to the published version of the manuscript.

Funding: This research was funded by the Russian foundation for basic research, grant number 20-45-596020.

Institutional Review Board Statement: Not applicable.

Conflicts of Interest: The authors declare no conflict of interest.

References

1. Prostański, D. Use of air-and-water spraying systems for improving dust control in mines. *J. Sustain. Min.* **2013**, *12*, 29–34. [CrossRef]
2. Yueze, L.; Akhtar, S.; Sasmito, A.P.; Kurnia, J.C. Prediction of air flow, methane, and coal dust dispersion in a room and pillar mining face. *Int. J. Min. Sci. Technol.* **2017**, *27*, 657–662. [CrossRef]
3. Voroshilov, Y.S.; Fomin, A.I. Impact of coal dust on the professional morbidity of coal industry workers. *Ugol* **2019**, *4*, 20–24. [CrossRef]
4. Liu, T.; Liu, S. The impacts of coal dust on miners' health: A review. *Environ. Res.* **2020**, *190*, 109849. [CrossRef]
5. Medvedev, I.I.; Krasnoshtein, A.E. *Aerology of Potash Mines*; Ural Branch of the Russian Academy of Sciences: Ekaterinburg, Russia, 1990. (In Russian)
6. Isaevich, A.G.; Shalimov, A.V.; Aleksandrova, M.A. Reduction of salt dust content in mining face and increase of the extraction ratio of chamber-mining method for a potash mine. *Bezopasnost' Truda v Promyshlennosti* **2021**, *12*, 37–43.
7. Williams, N. Potash ore and perforation of the nasal septum. *J. Occup. Med.* **1974**, *16*, 383–387.
8. Pahwa, P.; McDuffie, H.H. Cancer among potash workers in Saskatchewan. *J. Occup. Environ.* **2008**, *50*, 1035–1041. [CrossRef]
9. Xiu, Z.; Nie, W.; Yan, J.; Chen, D.; Cai, P.; Liu, Q.; Du, T.; Yang, B. Numerical simulation study on dust pollution characteristics and optimal dust control air flow rates during coal mine production. *J. Clean. Prod.* **2020**, *248*, 119197. [CrossRef]
10. Nie, W.; Wei, W.; Ma, X.; Liu, Y.; Peng, H.; Liu, Q. The effects of ventilation parameters on the migration behaviors of head-on dusts in the heading face. *Tunn. Undergr. Space Technol.* **2017**, *70*, 400–408. [CrossRef]
11. Xi, Z.; Jiang, M.; Yang, J.; Tu, X. Experimental study on advantages of foam–sol in coal dust control. *Process Saf. Environ. Prot.* **2014**, *92*, 637–644. [CrossRef]
12. Lu, G.; Hu, H.; Xing, F. Numerical Simulation Study on the Movement Characteristics of Dust Flow in Mine Working Face. *IOP Conf. Ser. Earth Environ. Sci.* **2019**, *384*, 012224. [CrossRef]
13. Wang, Z.; Ren, T.; Zhang, J. Numerical investigations of airflow patterns on a longwall face. *Int. J. Oil Gas Coal Technol.* **2020**, *24*, 321–344. [CrossRef]
14. Arya, S.; Novak, T.; Sottile, J. Experimental and Numerical Investigation of the Effect of Integration of a Flooded-Bed Scrubber into a Longwall Shearer on Airflow along a Coal Mine Longwall Face. *Appl. Sci.* **2021**, *11*, 3617. [CrossRef]
15. Semenov, V.V.; Fisunov, A.V.; Nikishin, I.O. Dynamic control system for mine ventilation. *IOP Conf. Ser. Mater. Sci. Eng.* **2021**, *1029*, 012090. [CrossRef]
16. Ren, T.; Wang, Z.; Cooper, G. CFD modelling of ventilation and dust flow behaviour above an underground bin and the design of an innovative dust mitigation system. *Tunn. Undergr. Space Technol.* **2014**, *41*, 241–254. [CrossRef]

17. Zhang, H.; Gu, W.; Li, Y.J.; Tang, M. Hygroscopic properties of sodium and potassium salts as related to saline mineral dusts and sea salt aerosols. *Res. J. Environ. Sci.* **2020**, *95*, 65–72. [CrossRef]
18. Kobylkin, S.S.; Timchenko, A.N.; Kobylkin, A.S. Use of computer simulation in the selection of operating parameters for the dust extractor built into the roadheader. *Bezopasnost' Truda v Promyshlennosti* **2021**, *3*, 21–27. [CrossRef]
19. Sapko, M.J.; Cashdollar, K.L.; Green, G.M. Coal dust particle size survey of US mines. *J. Loss Prev. Process. Ind.* **2007**, *20*, 616–620. [CrossRef]
20. Levin, L.Y.; Isaevich, A.G.; Semin, M.A.; Gazizullin, R.R. Dynamics of air-dust mixture in ventilation of blind drifts operating a team of cutter-loaders. *Gornyi Zhurnal* **2015**, *1*, 72–75. [CrossRef]
21. Vutukuri, V.S.; Lama, R.D. *Environmental Engineering in Mines*; Cambridge University Press: Cambridge, UK, 1986.
22. Fainburg, G.Z.; Isaevich, A.G. Analysis of microcirculation flows between microzones in face areas of blind shear stopes in potash mines with different ventilation methods. *MIAB Min. Inf. Anal. Bull.* **2020**, *3*, 58–73. [CrossRef]
23. Fainburg, G.Z.; Isaevich, A.G.; Zaitsev, A.V. Enhancement of ventilation efficiency in blind roadways of potash mines by dust criterion. *MIAB Min. Inf. Anal. Bull.* **2021**, *8*, 38–50. [CrossRef]
24. Song, C.H.; Carmichael, G.R. A three-dimensional modeling investigation of the evolution processes of dust and sea-salt particles in east Asia. *J. Geophys. Res. Atmos.* **2001**, *106*, 18131–18154. [CrossRef]
25. Kim, M.; Park, J.; Jo, Y.; Lee, D.; Yi, H. Numerical Investigation of Characteristics of Mine Ventilation Using One or Two Ducts in Underground Mining Faces. In Proceedings of the International Conference on Innovations for Sustainable and Responsible Mining, Hanoi, Vietnam, 15–17 October 2021.
26. Silvester, S.A.; Lowndes, I.S.; Kingman, S.W.; Arroussi, A. Improved dust capture methods for crushing plant. *Appl. Math. Model.* **2007**, *31*, 311–331. [CrossRef]
27. Kurnia, J.; Sasmito, A.P.; Mujumdar, A. Simulation of a novel intermittent ventilation system for underground mines. *Tunn. Undergr. Space Technol.* **2014**, *42*, 206–215. [CrossRef]
28. Zheng, Y.; Tien, J. DPM dispersion study using CFD for underground metal/nonmetal mines. In Proceedings of the 12th U.S./North American Mine Ventilation Symposium, Reno, NV, USA, 9–11 June 2008; pp. 487–494.
29. Aloyan, A. *Modeling the Dynamics and Kinetics of Gaseous Impurities and Aerosols in the Atmosphere*; Science Publishing House: Moscow, Russia, 2008. (In Russian)
30. Chernopazov, D.S.; Sekuntsov, A.I. Technological and geomechanical aspects of involving in the development of substandard by thickness sylvinite layers AB at the mines VKMKS. *JPME* **2013**, *12*, 47–56. [CrossRef]
31. Jones, W.P.; Launder, B.E. The Prediction of Laminarization with a Two-Equation Model of Turbulence. *Int. J. Heat Mass Transf.* **1972**, *15*, 301–314. [CrossRef]
32. Shih, T.H.; Liou, W.W.; Shabbir, A.; Yang, Z.; Zhu, J. A new k-e eddy viscosity model for high Reynolds number turbulent flows. *Comput. Fluids* **1995**, *24*, 227–238. [CrossRef]
33. Toraño, J.; Torno, S.; Menéndez, M.; Gent, M. Auxiliary ventilation in mining roadways driven with roadheaders: Validated CFD modelling of dust behaviour. *Tunn. Undergr. Space Technol.* **2011**, *26*, 201–210. [CrossRef]
34. Chen, D.; Nie, W.; Cai, P.; Liu, Z. The diffusion of dust in a fully-mechanized mining face with a mining height of 7 m and the application of wet dust-collecting nets. *J. Clean. Prod.* **2018**, *205*, 463–476. [CrossRef]
35. Semin, M.A.; Isaevich, A.G.; Zhikharev, S.Y. The Analysis of Potash Salt Dust Deposition in Roadways. *J. Min. Sci.* **2021**, *57*, 341–353. [CrossRef]
36. Van Leer, B. Toward the Ultimate Concervative Difference Scheme. IV. A Second Order Sequel to Godunov's Method. *J. Comput. Phys.* **1979**, *32*, 101–136. [CrossRef]